Fluid Mechanics
2021; 7(1): 9-16
http://www.sciencepublishinggroup.com/j/fm
doi: 10.11648/j.fm.20210701.12
ISSN: 2575-1808 (Print); ISSN: 2575-1816 (Online)

Effect of an Oscillating Grid on Hydrodynamics and Gas-liquid Mass Transfer in an Aquarium

Djimako Bongo[1, *], Nekoulnang Djetounako Clarisse[2], Jean-Yves Champagne[3]

[1]Mechanical Engineering Department, Higher Normal School of Technology of Sarh, Sarh, Chad

[2]Paleontology Department, National Research Center for Development of N'djamena, N'djamena, Chad

[3]Mechanical Engineering Department, Laboratory of Fluid Mechanics and Acoustics, INSA-Lyon, Lyon, France

Email address:

djimako.b5@gmail.com (D. Bongo)

[*]Corresponding author

To cite this article:

Djimako Bongo, Nekoulnang Djetounako Clarisse, Jean-Yves Champagne. Effect of an Oscillating Grid on Hydrodynamics and gas-liquid Mass Transfer in an Aquarium. *Fluid Mechanics.* Vol. 7, No. 1, 2021, pp. 9-16. doi: 10.11648/j.fm.20210701.12

Received: May 4, 2021; **Accepted**: June 1, 2021; **Published**: June 15, 2021

Abstract: This experimental study describes the effect of the oscillating grid on hydrodynamics and mass transfer in an aquarium. The contribution of the two driving elements CO2 and oscillating grid is identified. Depending on the operating conditions, either these two effects add up and promote the circulation and transport of the liquid, or these effects are opposite, the liquid velocity is then reduced. On the other hand, with regard to gas-liquid mass transfer, the use of the grid is beneficial since, under certain operating conditions; the mass transfer coefficient is increased compared to that obtained without the grid. Analysis of the various energy contributions in the unit shows that the presence of the grid is justified only in cases where the CO2 flow rate must remain low. Flow characterization was performed using Particle Image Velocimetry (PIV) technique. The results were compared with previous studies. In order to perform the concentration field measurements by planar laser induced fluorescence (PLIF) technique and simultaneous PIV and PLIF measurements, the test bench was modified. The observations of velocity and concentration fields are in adequacy with the previous studies and allow to validate the bench. The necessary tools have been put in place, the study of mass transfer can continue.

Keywords: Hydrodynamics, Oscillating Grid, Mass Transfer, Velocity Fields, Concentration Fields, PIV-PLIF

1. Introduction

The optimal design of two-phase aquariums requires a great deal of knowledge in chemistry, mass or heat transfer, or in terms of the flow of circulating phases. Their principle of operation is simple. They consist of a column connected at their lower and upper ends. Inside, the injected gas causes a variation in density. The circulation is thus ensured with an ascending gas-liquid flow in the column. These devices allow to work in important speed ranges ensuring a very satisfactory exchange between phases (gas-liquid) and improving productivity performances. They can be used in a wide range of industrial applications such as the continuous production of citric acid or the culture of different types of yeast or bacteria [1] or the growth of microalgae [2]. Liquid circulation and CO_2-water mass transfer are essentially dependent on the gas flow rate in the aquarium. In this case, in order to maintain good liquid circulation conditions, an oscillating grid can be considered. The installation of a stirring system at the bottom of the aquarium allows the particles to be suspended and ensures good homogeneity. The objective of the study is to identify the hydrodynamic and mass transfer characteristics and then the determination of velocity fields by the PIV method and CO_2 concentration fields by PLIF.

2. Description and Principle

The test bench must achieve homogeneous and isotropic turbulence within the fluid Figure 1. Firstly, the supply and storage of the two fluids must be easy and safe. For this purpose, access must be provided to fill the tank and static and dynamic seals must be ensured. To carry out different tests, the grid oscillation must be constant and reproducible. The amplitude and frequency of the oscillation must allow

the mass transfer phenomenon to be studied over a wide range of turbulence. The various measurements of flow and concentration must be able to be made at any point in the vessel.

The frame of the test bench is made of ELCOM 40x40 aluminium profiles. Brackets are used to connect the different parts together. Tests have shown a vibration of the bench when used at high frequencies. In order to stabilise it, the test stand is now mounted on ELCOLM stands. The components of the optical measuring chains (laser sheet generation, camera...) are directly assembled on the bench in order to facilitate the positioning of the measuring planes and to ensure its good repeatability. A matt black fabric is placed behind the tank in order to guarantee a neutral and homogeneous background. This allows, among other things, to avoid certain reflections. The internal dimensions of the cell are 277x277x550 mm or 3.07.10-2m^3. The side walls and the lid of the tank are made of Plexiglas to allow the passage of laser rays through the tank during experimental measurements and are 20 mm thick. The bottom of the cell is used for positioning, fixing and sealing of the cell walls. It also ensures the mounting and alignment of the guides for the translation of the grid, and the installation of the pH and CO_2 probes. In addition, it allows the entry of N2 gas and water. It is therefore an essential part of the device.

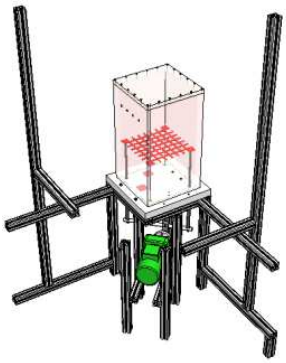

Figure 1. *Test bench.*

Figure 2. *Tank bottom.*

The test bench is equipped for the simultaneous measurement of all three quantities:

Measurement of velocity fields at the bottom of the tank and near the air-liquid surface PIV) - Measurement of CO_2 concentration in a near-surface gas-field of view- liquid (PLIF).

Measurement of the average CO_2 concentration with a CO_2 probe at the bottom of the tank.

3. How the Aquarium Works

The mass transfer results from the hydrodynamics, specifically the flow conditions in the aquarium and the total exchange area. The main hydrodynamic characteristics of an aquarium are the retentions of each phase, the flow speed of the liquid, the mixing time. These quantities depend on the operating conditions of the studied system: the geometrical characteristics of the aquarium, the gas flow rate, the oscillation frequency of the grid. The influence of the gas velocity, which is generally the main operating parameter, is a fundamental data. Increasing the gas flow rate, which accelerates the circulation of the liquid, leads to the entrainment of bubbles in the aquarium and thus increases gas retention. The speed of liquid circulation plays a major role in turbulence phenomena and mass transfer. As with gas retention, the nature of the liquid, the presence of CO_2, the viscosity of the medium or the geometry of the system influence the circulation of the liquid. Several correlations are proposed but one of the most used is the one of [3] established from an energy balance on the reactor. For this type of reactor, the complete suspension of particles is ensured if the gas velocity is above a threshold called critical gas velocity. The installation of a bottom stirring system will allow a suspension of the particles even if the critical gas velocity is not reached. In addition, several studies have also been carried out using a mechanical stirring system either in a bubble column [4], a gas-liquid stirred reactor [5] or an airlift column [1]. In the case of a self-suction agitated reactor, previous works [6, 7] tested the performance of several agitation systems and showed that the power dissipated by the agitator decreases in the presence of gas, whatever the agitation system studied. In an internal loop reactor, previous study [5] showed that by using an axial flow stirrer, liquid circulation is improved and mixing time is reduced. Finally, concerning mass transfer, [1] measured the influence of the speed of an agitator (Rushton turbine) on the gas-liquid mass transfer as it was done in a stirred vessel. The mass transfer coefficient kLa depends on the gas injection conditions but also on the stirring conditions. These authors propose a general correlation of the type:

$$k_L a = \alpha(\frac{P_A}{V})^{\alpha}(\frac{P_{ag}}{V})^{\beta} \quad (1)$$

3.1. Method

Prior to image acquisition, the laser sheet is adjusted so that it passes through the cell at the level of the markings indicating the measuring plane Figure 3. The optics must be focused in order to have the thinnest possible sheet and to have a high intensity in the center of the cell. When adjusting the camera, make sure that the camera is levelled and check the perpendicularity of the lens to the laser plane. A calibration with a test rod immersed in the cell and placed in

the laser plane is carried out before each change of configuration. This makes it possible to check the positioning of the camera and to find the relationship between the coordinates in the image and the coordinates in the measurement plane. It thus makes it possible to determine the ratio: distance in pixels on the image - actual distance in meters. An optical filter is placed in front of the camera in order to let pass only the wavelength of the laser beam λ = 532 nm. From the acquired images, the operations of background subtraction and mask application lead to an increase in the signal-to-noise ratio and to the determination of the instantaneous velocity fields. Subsequently, using statistical methods, residual noise vectors can be identified and eliminated. To obtain a background image, two methods were used. The first is to take a series of images of the flow illuminated by the laser sheet, without seeding the crystals. The second is to average the images obtained with the seeding. Both techniques give similar results. During an acquisition test, the aperture of the diaphragm and the intensity of the laser are fixed so as not to saturate the sensor. In practice, the aperture is set at maximum to have a shallow depth of field and observe only the particles in the slick, and then the laser power is adjusted so as not to saturate the camera sensor. Then, during a continuous acquisition test, the camera must be focused: the particles illuminated by the laser plane must appear clearly in the images. Before all measurements, the tank is cleaned, filled and seeded with particles. The tracers used for the PIV are hollow glass beads with a diameter of 10 µm. The grid was set in oscillation at least 20 minutes before imaging. For this study, the entire flow is visualized on the image. These vectors were obtained with 12x12 pixel query windows with 50% overlap. The time-averaged velocity fluctuations u^' and v^' are the RMS of 600 or 1000 instantaneous velocity fields. The time interval between the two images is chosen according to the oscillation frequency of the grid and thus the flow velocity in order to have an average particle displacement approximately equal to 1/3 of the interrogation window. For example, for a low grid oscillation frequency of 1 Hz, the time interval between laser pulses is 19822.2 µs.

Figure 3. *PIV laser beam mounting.*

3.2. Principle of PLIF

Laser plane-induced fluorescence is a non-intrusive process for measuring a scalar field. The technique is composed of a light source (laser plane), and a scalar emitting photons, under the effect of the source by fluorescence, captured by the acquisition system (camera). Fluorescence is an atomic excitation process during which a photon is emitted with a wavelength longer than the excitation Figure 4 [8].

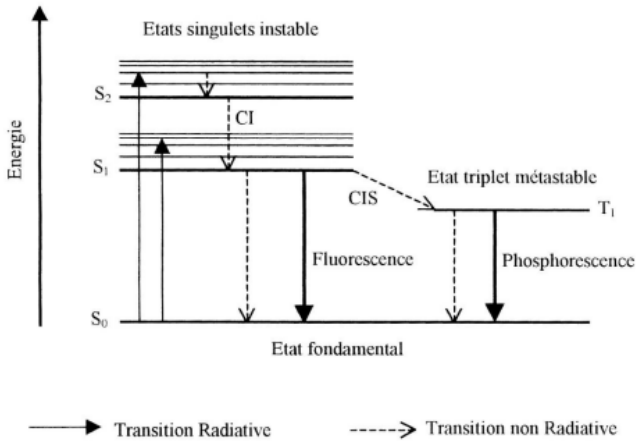

Figure 4. *Energy levels.*

In this study, the PLIF is used to measure the CO_2 concentration fields in the tank. This CO_2 concentration is determined from the light intensity emitted by the sodium fluorescein [9]. The scalar must therefore have a fluorescence property in relation to the amount of CO_2 present. Sodium fluorescein was chosen for its sensitivity to pH Figure 5. This quantity is then used for the determination of the CO_2 concentration.

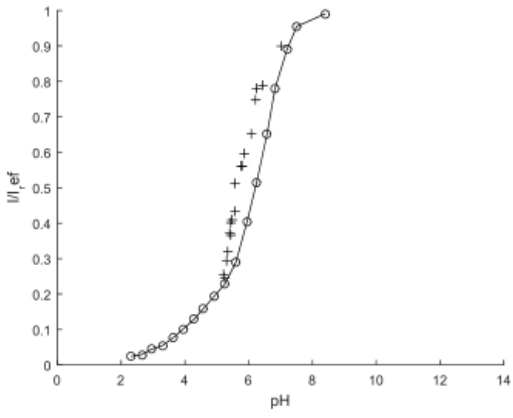

Figure 5. *Curve I- pH.*

Indeed, the chemical reaction of CO_2 and water leads to the formation of carbonic acid and thus to a decrease in pH Figure 6. The light intensity re-emitted by the sodium fluorescein is inversely proportional to the concentration of CO_2. Figure 6 [10] represents this correspondence. The data were obtained with a Metler Toledo CO_2 InPro 5000 sensor.

The empty points correspond to CO_2 concentrations below the manufacturer's specifications (14.7 mg/L).

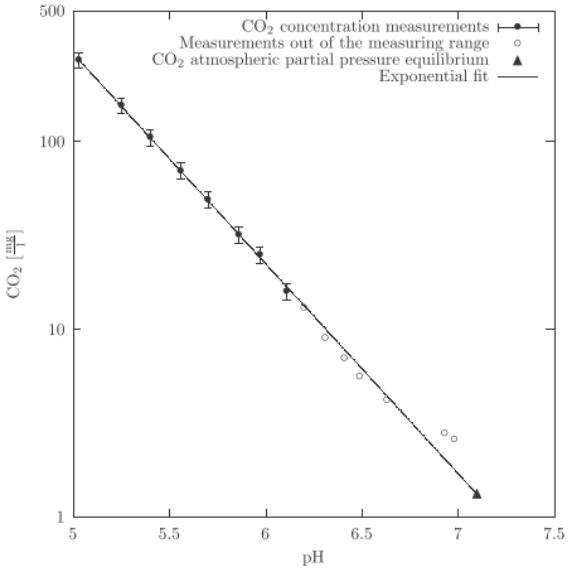

Figure 6. *CO_2-pH curve.*

3.3. Principle of PIV

Particle Image Velocimetry is an optical method of determining the velocity of a fluid from the motion of particles carried by it. This technique makes it possible to reconstitute a velocity field in a plane by dividing the images into query windows and determining the velocity of the particles located in them. The main difference between PIV and other techniques such as Velocimetry or Laser Doppler Anemometry is that it allows obtaining a large vector field in two or three dimensions. The other techniques are point methods.

By taking two images of the flow, spaced by a very short time and calculating the distance travelled by tracer particles during this time, the velocity can be calculated using image processing software. At present, optical techniques are preferred for turbulence measurements because the sensor is located outside the flow. They are said to be non-intrusive and do not disturb the flow. Seeding of the flow is carried out with sodium fluorescein at a concentration of 3.61.10-7mol.L-1 and a concentration of 0.1g.L-1 of spherical glass particles of 10µm diameter (HGS-10) for PIV. Image and velocity field processing is performed in the same way as the separate PIV and PLIF measurements. Superimposition and analysis of the acquisitions can be performed by DaVis and Matlab software.

4. Results

The images are taken by means of an image doubler (Figure 7). This allows the image of the flow to be duplicated and each image is projected onto one-half of the camera sensor. A first image is obtained after passing through a band pass filter λ = 488 nm in order to record the displacement of the particles at different times for the calculation of velocity fields by PIV. For the second image, a high-pass filter λ = 520 nm is used in order to let only the fluorescent light pass through and thus block the light of the particles. This image will be used to obtain the CO_2 concentration fields by the PLIF technique.

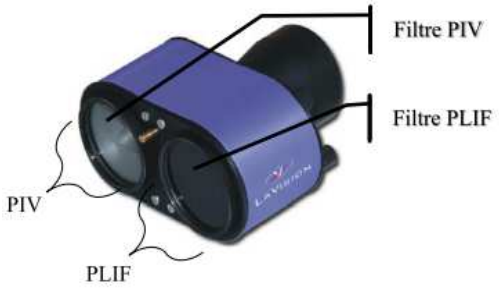

Figure 7. *Image doubler.*

The image doubler can only be attached to a 50 mm lens, resulting in a small aperture angle. A target system Figure 8 is placed in the laser plane in the center of the cell to allow calibration. The two obtained images can be superimposed Figure 9. The use of a doubler reduces the light intensity of the acquisitions. This has an influence on PIV and PLIF measurements. It is therefore necessary to concentrate the beam in a reduced area. In addition, the particles create local shadows and therefore vary the light intensity.

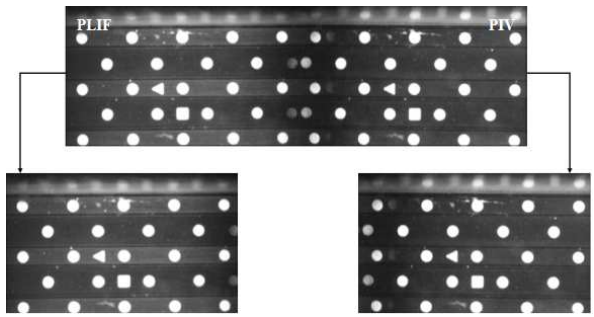

Figure 8. *Sight system.*

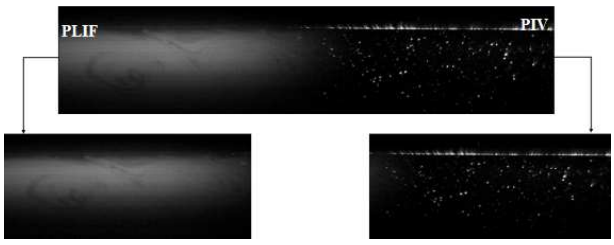

Figure 9. *Gross acquisition PIV | PLIF.*

4.1. Influence of the Water Level

The average speeds were found to be approximately the same. Only the profile of the mean velocities in Figure 10.(1), with the lowest water height of 150 mm, shows a slightly different profile. This can be explained by the fact that recirculation is directly blocked by the surface. This blocking results in a change in the flow profile.

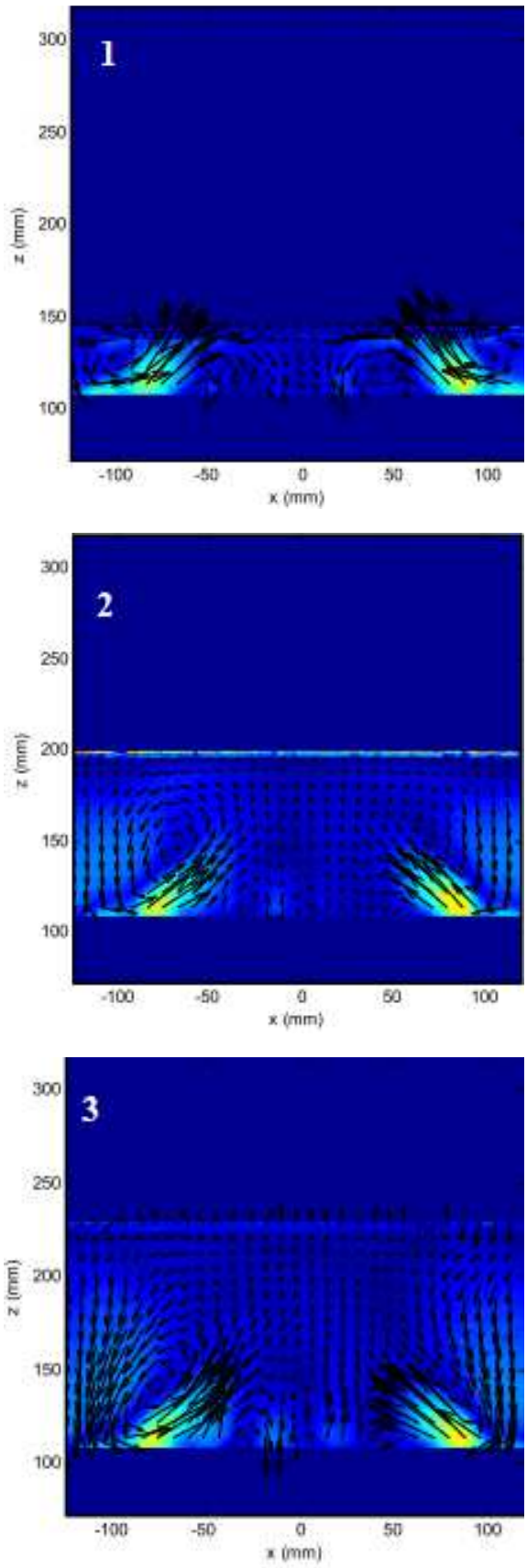

Figure 10. *Velocity fields under the influence of water level.*

The profile of the velocity field measurements in Figure 10. (1) is, slightly different from the other two. This conclusion is consistent with the general observations of grid turbulence. Indeed, the turbulence becomes homogeneous from a certain distance from the grid. For the velocity measurements in Figure 10. (1), the water height is less than the distance required for homogenization of the flow. The turbulence in this area depends on the displacement of the oscillating grid. As determined theoretically, it is necessary to have a water head greater than the distance sufficient to achieve homogeneous turbulence. Once this condition is met, the water height shows no significant influence on the velocity fields as in [11] Figure 10. (2) and (3).

4.2. Influence of the Oscillation Frequency

The analyses give similar results in terms of flow profile. Averaging the instantaneous velocity fields gives the same structures. Nevertheless, the intensity of the velocities varies with the oscillation frequency of the grid. The velocity of fluid ejection towards the center is more intense Figure 11.(3).

PLIF results show that the first darker layer at the interface appears when the CO_2 concentration reaches saturation. In the area directly below the interface, the thin layer shows the rapid decrease in concentration. Below the boundary layer, the lighter images indicate an area of low CO_2 concentration that is constantly mixed by the turbulence generated by the oscillating grid. Figures 12.(1), 12.(2) and Figure 12.(3) show the instantaneous concentration fields in relative grey scale, respectively. The dark to light color scale corresponds to areas of high and low CO_2 concentration, respectively.

It is interesting to observe the influence of the action of turbulent structures in the instantaneous concentration field images.

By the same principle, it is possible to visualize the instantaneous concentration profile as a function of the x position. This makes it possible to study, in more detail, the structures present, at the same time, at the interface. Figures 13, 14, 15 present the instantaneous concentration profiles from the concentration field. The CO_2 concentration is expressed, here, in mg/L. The peeling process is highlighted by local differences in concentration.

4.3. Influence on Dissolution

Figure 15 shows the instantaneous CO_2 concentration field represented in grayscale. Black corresponds to regions with high CO_2 concentration and light grey to low concentration. In the vicinity of the interface, a thin layer corresponds to the diffusional boundary layer according to [12], which is very thin. Beyond this layer, the CO_2 concentration decreases rapidly, the images are dominated by a light color corresponding to a low CO_2 concentration in the region permanently affected by the turbulence generated by the oscillating grid. Note that the presence of regions of high concentration corresponding to CO_2 dragged towards the bottom by the eddy structures is the peeling phenomenon [12, 13].

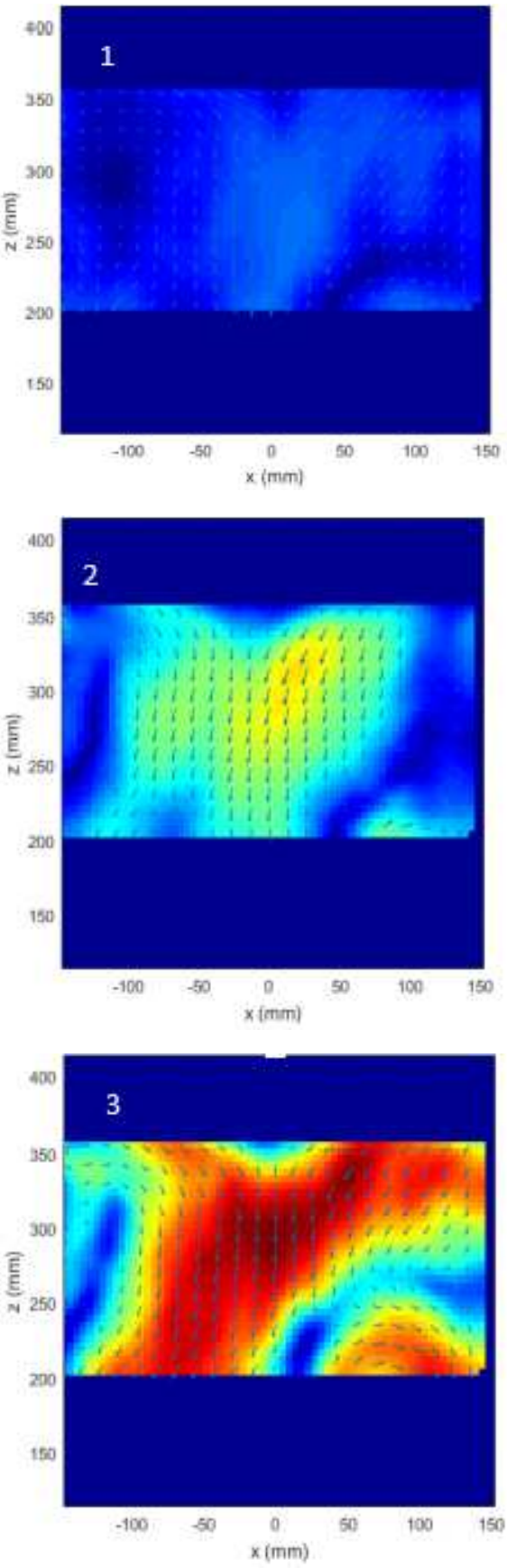

Figure 11. *Velocity fields under the influence of oscillation frequency.*

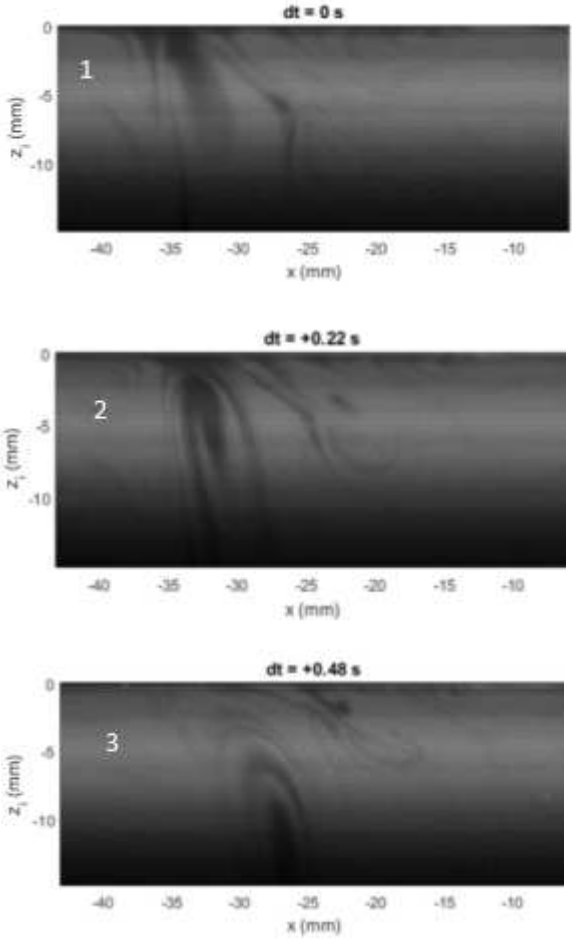

Figure 12. *Influence of time on the dissolution of CO_2.*

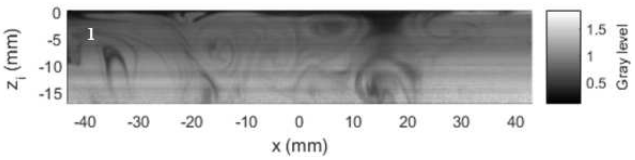

Figure 13. *PLIF Processing | Normalized Image Intensity.*

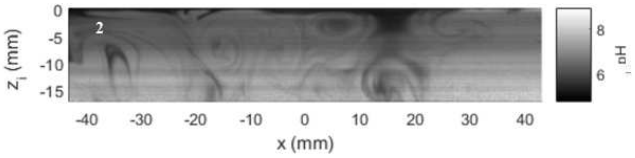

Figure 14. *PLIF treatment pH influence.*

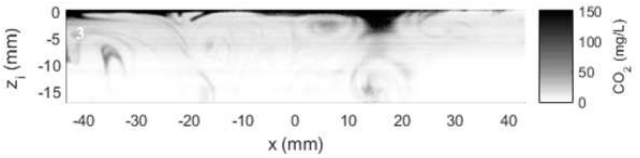

Figure 15. *PLIF treatment, CO_2 concentration.*

These observations show that the dissipation of the turbulence plays a major role in the transfer of gas across the gas-water interface. The rate at which CO_2 is transported across the interface, where the liquid is in turbulent motion, is determined by the thickness attained by the viscous

boundary layer [13], with reference to the conventional solid wall plate boundary layer [15] under the action of turbulence and at what rate the turbulent structures replace the CO_2-laden liquid near the surface with liquid of low CO_2 content.

4.4. Coupled Velocity and Concentration Measurements

Figure 16, DaVis 8.1.2 shows three (3) successive acquisitions of CO_2 velocity and concentration fields. The superimposition of these two measurements allows a better understanding of the contribution of turbulence on the mass transfer at the interface. The transport of fluid with high CO_2 concentration is associated with the vortex structure approaching the surface.

Figure 16 also demonstrates the correspondence between the velocity and concentration fields. This confirms that the PIV and PLIF acquisitions have, therefore, been obtained simultaneously in time and space. The velocity and concentration fields are explored simultaneously using PIV and PLIF [15] in order to determine the relationship between the hydrodynamics in the liquid phase and the coefficient KL.

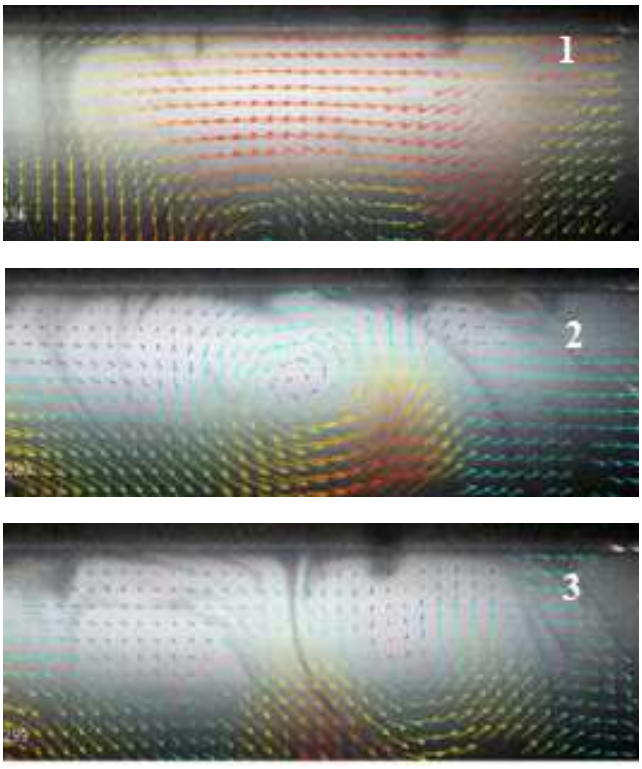

Figure 16. *Coupled PIV-PLIF visualization.*

5. Conclusion

This parametric study of a column with an oscillating grid allowed to understand the hydrodynamics of this aquarium and to quantify the beneficial effect of the mechanical oscillation of the grid on the liquid circulation and on the mass transfer. This aquarium makes it possible to operate in a two-phase environment with particles of large size and density. Moreover, in agitated media, mass transfer is not only linked to gas retention. The oscillation system modifies the flow around the gas bubbles thus increasing the transfer coefficient. In order to increase our knowledge of the fundamental physical mechanisms controlling mass transfer, it is necessary to characterize the hydrodynamics of the flow and the different contributions to the total flow. First, the flow characterization was carried out using the PIV technique. The results were compared with previous studies. In order to perform concentration field measurements using the PLIF technique and simultaneous PIV-PLIF measurements, a doubler was used. Initial observations of the rate and concentration fields are consistent with previous studies and serve to validate the results.

6. Recommendations

The test bench and the techniques are now operational. In order to continue this study, it is advisable to repeat the series of mentioned measurements, in order to fully control the different means of measurement. Afterwards, it may be interesting to modify more deeply the different parameters of turbulence creation and measurement.

References

[1] Barru, B., et al. (2011) Mass Transfer Efficiency of a Vacuum Airlift—Application to Water Recycling in Aquaculture Systems. Aquacultural Engineering, 46, 18-26.

[2] Siegel, M. H. and C. W. Robinson, "Applications of Airlift Gas Liquid Solid Reactors in Biotechnology", Chem. Eng. Sei. 47, 3215-3229 (1992).

[3] Barrut, B. (2011) Etude et optimisation du fonctionnement d'une colonne airlift à dépression—Application à l'aquaculture. 137 p.

[4] Dutta, N. N. and V. G. Pangarkar, "Critical Impeller Speed for Solid Suspension in Multi-impeller. Three Phase Agitated Contactors", Can. J. Chem. Eng. 73, 273-283 (1995).

[5] Favre, E., M. Derond and P. Peringer, "Influence of a Rotating Sieve on Pumping and Mixing Performances in an [ntemal Loop Reactor", Bioprocess Engineering 11, 91-95 (1994).

[6] Nguyen, C., "Etude et comparaison de trois contacteurs gaz liquide à auto-aération", Thèse de Doctorat INPL, Nancy, France (1993).

[7] Anastassiades, E., "Etude du fonctionnement de mobiles autoaspirants dans les réacteurs agités gaz liquide", Thèse de Doctorat INPL, Nancy, France (1995).

[8] J. G. Janzen et al.: Estimation of mass transfer velocity based on measured turbulence parameters. AIChE Journal, 56 (8): 2005–2017, 2010, ISSN 1547-5905.

[9] P. Valiorgue, N. Souzy, M. El hajem, H. Ben hadid, S. Simoens "Concentration measurement in the wake of a free rising bubble using planar laser-induced fluorescence (PLIF) with a calibration taking into account fluorescence extinction variations", Exp. Fluids 54, 1501.

[10] N. Souzy: Experimental study and improvement of mass transfer in vertical bubble columns. Thèse de doctorat, Université Claude Bernard Lyon 1, (2014).

[11] N. Matsunaga et al Quantitative properties of oscillating-grid turbulence in a homogeneous fluid, Fluid dynamics research 25.3: 147-165, (1999).

[12] H. HERLINA, "Gas transfer at the air-water interface in a turbulent flow environment", Thèse de doctorat, Université de Karslruhe, (2005).

[13] E. A. Variano & E. A. Cowen, “Turbulent transport of a High-Schmidt-number scalar near an air-water interface”, J. Fluid Mech., vol. 731, pp. 259-287, (2013).

[14] J. C. Hunt & J. M. R. Graham, “Free-stream turbulence near plane boundaries”, J. Fluid Mech., 84, part 2, pp. 209-235, (1978).

[15] Cheng, Nian-Sheng, and Adrian Wing-Keung Law. "Measurements of turbulence generated by oscillating grid." Journal of Hydraulic Engineering 127.3: 201-208, 2001.